# miniRadar: A Low Power IEEE 802.15.4 Transceiver Based Implementation of Bistatic Radar

Pradipta Ghosh
University of Southern California
Los Angeles, CA, USA
pradiptg@usc.edu

Jenny Xie
Wellesley College
Wellesley, MA, USA
jxie2@wellesley.edu

Bhaskar Krishnamachari
University of Southern California
Los Angeles, CA, USA
bkrishna@usc.edu

## ABSTRACT

We present a proof-of-concept low-power IEEE 802.15.4 standard based bistatic radar system for localizing unknown radio-wave reflecting objects in an unknown environment. Unlike prior multi-antenna based approaches, we employ a single standard low power omnidirectional transmitter with known transmission parameters and a single rotating directional receiver antenna to collect a set of directional RSSI samples and, thereafter, exploit the directionality information of the samples to determine the locations of the reflecting objects. To this end, we employ the well-known Maximum Likelihood Estimator (MLE) to extract required information from the collected RSSI samples. To test the concept, we have developed a real hardware prototype of the system. Through a set of simulation and real experiments, we demonstrate the potential of the proposed concept. To our knowledge this is the first bistatic radar system demonstrated with low cost low power off-the-shelf 802.15.4 radios.

## CCS CONCEPTS

• **Computer systems organization → Sensors and actuators**;

## 1 INTRODUCTION

Over last decade, Radio Frequency (RF) signal based sensing has become very popular among researchers due to its ubiquitous nature and wide range of applicability. Researchers have applied RF signal in many sensing and mapping contexts including but not limited to robotic mapping of unknown areas [10], indoor localization [9], and see through capabilities [11]. Radio Signal Strength Information (RSSI) is one of the most useful and ubiquitous property of RF signals. In this work, we propose a low-power RSSI-based bistatic radar [19] system implemented with IEEE 802.15.4 radios to localize a set of unknown radio-wave reflecting physical objects in a deployment environment. A bistatic radar [19] is a well known RF system that is composed of a transmitter and a receiver separated by a large distance compared to the distance to an object. A bistatic-radar employs the difference in the path lengths travelled by a direct path signal and a multipath signal reflected by an object to passively localize the object.


*HotWireless'17, October 16, 2017, Snowbird, UT, USA*

ACM ISBN 978-1-4503-5140-9/17/10…$15.00
https://doi.org/10.1145/3127882.3127891

One motivation for our investigation into building a bistatic radar using commercial off-the-shelf low-power radio devices is that conventional radar systems are expensive, incur high computation, and have high power consumption (e.g., even low power radars such as for automotive systems consume $\geq$ 2.5 Watts). We aim to implement a low-power bistatic radar through our proposed system that can be used for scanning and monitoring dynamic indoor environments. Moreover, our proposed system is mounted on a moving controllable robot that can move and scan an unknown environment. Using a 802.15.4 radio has advantages over conventional radar because it is low-power ($\sim$ 10 mW), smaller in size, and low-cost. However, RSSI based mapping is often deemed difficult and erroneous in indoor environments due to presence of multipath components [15, 16]. Instead of viewing multipath as a detriment, our work focus on separating the multipath components and use them to find the reflecting objects in a manner similar to a bistatic radar.

RF signal based localization and mapping have been extensively studied in the existing literature. In this context, the work of Mostofi *et al.* [7, 11] on mapping of an environment using two moving RF transceivers robots is relevant. In their works, the robots follow a predetermined set of paths for collecting a set of RF samples which are later processed using the concept of compressible sampling to map obstacles. They exploit the attenuation introduced by different obstacles to map them. *Our goal is slightly different as we are interested in passively localizing the objects/surfaces by extracting multipath components from the received signal at a single receiver while the transmitter and receiver remain in line of sight with respect to each other. This also separates our work from the standard RF Sensor Network based passive localization works [14] where a fixed network of RF devices monitor changes in the RF communication channel properties in order to passively localize an object.* There also exist some passive localization works that employ UWB radios and MIMO systems to localize objects. Aditya and Molisch [3] presented one such solution where a set of transmitters and receivers use the blocking characteristics of pairwise communication links to passively localize objects. Gulmezoglu, Guldogan, and Gezici have proposed a similar UWB radio based solution in [6]. There also exist some works that use RFID [18] and multiple receiving antennas for localization. The work of Tan, Chetty, and Jamieson [17] on using 8-element uniform circular phased arrays for through-wall passive sensing and mapping is also relevant. The proposed system, called TrueMapper, was built on top of costly, power consuming USRP radios. Fadel *et al.* [1, 2] have worked on a custom solution called RF-capture that employs a directional antenna array to sense human motions. They capture the reflections off a human body with each antenna transceiver in the array, which are later processed jointly to generate an image. Chetty, Smith, and Woodbridge [5] also presented a wifi based multi-static radar system for through-the-wall passive sensing. There also exist some systems [8] that use phase information of the RF signal along with RSSI to implement synthetic aperture radar (SAR) based imaging and localization. However, most of the cheap, commercially available RF modules do not provide access to the phase information. *What separates our work is the application of a single RF transmitter-receiver antenna pair instead of multiple antennas or antenna arrays to achieve passive localization of reflecting objects with acceptable performance that can be implemented with low-cost off-the-shelf hardware.*

In this proof-of-concept work, we propose a system with a single rotating directional antenna that scans the environment for different orientation of the antenna and collects a set of directional RSSI samples from a single omnidirectional transmitter. Next, we feed these directional RSSI samples in form of a RSSI vector to a MLE based estimation module that iterates through different potential combinations of the transmitter and reflectors locations to find the location combination that is most probable to generate the collected RSSI vector. Currently, the processing of the signal is executed offline in MATLAB. However, in future, we aim to achieve the processing in a commercially available sensor motes such as Openmote [12] platform. We also developed a prototype system on top of a controllable robot with the vision that in future the sensing system with controlled motion can achieve a low-complexity, better granularity passive localization and mapping compared to the multiple antenna based systems. We performed a set of simulation and real-world experiments to prove the concept and to analyze the performance of the MLE based estimation algorithm. Our results suggest that the errors in the position measurements of the reflectors are lower when the distance between the transmitter-receiver pair ($d$) is either comparable or higher than the distances between the reflectors and the receiver ($d_o$). This is attributable to the fact that for a closely spaced transmitter-receiver pair the direct-path component is too strong compared to the multipath components.

## 2 PROBLEM FORMULATION

In this section, we explain the problem formulation and our proposed system design in details. Let there exist a set of $N$ reflecting **point objects**[1] in a 2D unknown environment with known dimensions, say $D_G \times D_G$ square region. Denote the location of the point reflectors as $\mathbf{X}_{\mathcal{R}} = \{X^i_{\mathcal{R}} = (x^i_{\mathcal{R}}, y^i_{\mathcal{R}}) | i = 1, \cdots N\}$. Our objective is to estimate the unknown $N$ and also the unknown location set $\mathbf{X}_{\mathcal{R}}$.

Our proposed system consists of a single directional antenna based receiver ($R_x$) with known gain pattern, $\mathbf{g_a} = \{g_{(-180+i\cdot\delta)} : i \in \mathbb{Z} \text{ and } i \in [0, 360/\delta)\}$ where $\delta$ is the angular scanning granularity and $g_{(\phi)}$ refers to the antenna gain along $\phi$ direction, and a single omnidirectional antenna based transmitter ($T_x$). Now, let the environment be modelled as a 2D discrete grid space with origin at the receiver location and positive y-axis direction of the 2D space being the $0^\circ$ orientation of the receiver. The length of a side of each grid ($d_G$) is a parameter to control the granularity of the estimation. The number of grid point is $n_G^2$ with the set of locations denoted as $\mathbf{X}_G = \{X^i_G = (x^i_G, y^i_G) | i = 1, \cdots n_G^2\}$. Let us assume that the reflector locations and the transmitter location are restricted to the set of the grid points, $\mathbf{X}_G$. Let us also denote the locations of the transmitter and the receiver as $X_{T_x}$ and $X_{R_x}$, respectively, and the distance between the $T_x$-$R_x$ pair as $d$. The directional rotating receiving antenna collects a set of RSSI samples[2] for different angular orientation of the antenna, starting from $-180^\circ$ (orientation toward negative y axis of the 2D reference frame) to $180^\circ$ in steps of $\delta^\circ$, to generate a RSSI vector, $\mathbf{r_o} = \{r_{(-180+i\cdot\delta)} : i \in \mathbb{Z} \text{ and } i \in [0, 360/\delta)\}$. This RSSI vector is used by the proposed MLE based reflector localization algorithm, detailed in Section 3.

For the wireless channel modelling, we use standard log-normal fading model [16]. For directional antenna, the model can be described as follows.

$$P_{R_x}(\theta) = C.g_{(\theta)}.P_{T_x}.10^{\Psi/10} \cdot d^{-\gamma}_{(\theta)} \tag{1}$$

where $P_{R_x}(\theta)$ is the received signal power along direction $\theta$ with respect to the antenna orientation, $g_{(\theta)}$ is the directional gain of receiving antenna, $C$ is a constant, $P_{T_x}$ is the transmitter power, $d_{(\theta)}$ is the distance travelled by signal incident along angle $\theta$, $\gamma$ is the path loss exponent, and $\Psi \sim \mathcal{N}(0, \sigma^2)$ is the log normal fading noise with variance $\sigma^2$. If the signal is a reflected signal, there will be some attenuation by the reflecting object which we denote by $\mathcal{A}(\kappa)$, where $\kappa$ is the angle of incidence on the reflecting object. However, for simplicity we take a constant value $\mathcal{A}$ as the attenuation constant. Also note that the coefficient of reflection is just 1 for the direct path component. Now, for each orientation of the receiver antenna, say, $\theta_o$ with respect to positive y-axis, the measured RSSI is actually a sum of different multipath components and can be represented as follows.

$$r'_{\theta_o} = \sum_{\theta \in [-180^\circ, 180^\circ)} C.\mathcal{A}.g_{(\theta-\theta_o)}.P_{T_x}.10^{\Psi/10} \cdot d^{-\gamma}_{(\theta)} \tag{2}$$

where $\theta$ actually signifies the angle of the multipath component with respect to the positive y axis (i.e, the rotating antenna's base orientation). Now using (2) for each possible set of reflector locations, $\mathbf{X}_{\mathcal{R}}$, and transmitter location, $X_{T_x}$, we can mathematically estimate the resulting RSSI vector as $\mathbf{r_v} = \{r'_{(-180+i\cdot\delta)} : i \in \mathbb{Z} \text{ and } i \in [0, 360/\delta)\}$. **Now the objective can be summarized as follows:** *find the most likely location set $\mathbf{X}_{\mathcal{R}}$ such that, for a known (or unknown) location of the transmitter $X_{T_x}$, the probability $\mathbb{P}(\mathbf{r_v} = \mathbf{r_o})$ is the highest, where $\mathbf{r_o}$ is the RSSI observation vector and the cardinality of the set $\mathbf{X}_{\mathcal{R}}$ i.e., $N$, is also unknown.*

## 3 MAXIMUM LIKELIHOOD ESTIMATION

In this section, we describe our maximum likelihood estimation [4] based approach for localizing a set of reflector objects. First, let us simplify the problem by restricting our focus to a single reflector scenario with known transmitter location, $X_{T_x}$. Next, we calculate the log likelihood of each of the grid point $X^i_G$ to be the reflector location, $X_{\mathcal{R}}$, as follows:

$$\begin{aligned} \log \mathcal{L}(\mathbf{r_o} | X_{\mathcal{R}} = X^i_G, X_{T_x}) \\ = \sum_{\theta_o \in [-180^\circ, 180^\circ)} \log \mathbb{P}(r'_{\theta_o} = r_{\theta_o} | X_{\mathcal{R}} = X^i_G, X_{T_x}) \end{aligned} \tag{3}$$

where we use Eqn (2) to estimate the probability $\mathbb{P}(r'_{\theta_o} = r_{\theta_o} | X_{\mathcal{R}} = X^i_G, X_{T_x})$. Then we choose the grid position with the maximum

[1] For simplicity, we ignore the dimensions of the reflecting objects and represent them by the points of reflection on the objects.

[2] We do not employ the RF phase information as it is not readily available (unlike RSSI) in most of the cheap, low power off-the-shelf radios.

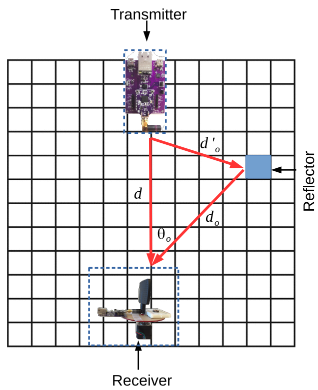


**Figure 1: Illustration of our bistatic radar equivalent system**

value of the likelihood function as the estimated reflector location.

$$X_{\mathcal{R}} = \underset{X_G^i}{\arg\max} \log \mathcal{L}(\mathbf{r_o} | X_{\mathcal{R}} = X_G^i, X_{T_x}) \tag{4}$$

This requires $\mathbb{O}(n_G^2)$ numbers of likelihood estimations where the number of grid points, $n_G^2$, depends on the search granularity, $d_G$, and the size of the environment, $D_G$. Now, if the location of the transmitter $X_{T_x}$ is also unknown, the MLE formulation can be written as follows.

$$\begin{aligned}\{X, X_{T_x}\} &= \underset{\{X_G^i, X_G^j\}}{\arg\max} \log \mathcal{L}(\mathbf{r_o} | X_{\mathcal{R}} = X_G^i, X_{T_x} = X_G^j) \\ &= \underset{\{X_G^i, X_G^j\}}{\arg\max} \sum_{\theta_o \in [-180°, 180°)} \log \mathbb{P}(r'_{\theta_o} = r_{\theta_o} | X_{\mathcal{R}} = X_G^i, X_{T_x} = X_G^j)\end{aligned} \tag{5}$$

where $i, j \in \{1, n_G^2\}$. This requires $\mathbb{O}(n_G^4)$ numbers of likelihood estimations. Generally speaking, **for a known number of reflectors (**$N$**)**, the MLE based approach iterates through different subsets of the grid points, $X_G$, as the possible set of the transmitter and reflector(s) locations and calculates the likelihood probability of the observation vector $\mathbf{r_V}$. Through comparing these likelihoods of the measured RSSI vector, we obtain the most likely location set for the reflectors and the transmitter. Now, **if** $N$ **is also unknown**, we need to perform likelihood for a range of values of $N$ as well. In such contexts, the MLE formulation can be expressed as follows.

$$\begin{aligned}\{X, X_{T_x}, N\} &= \underset{\{\mathbf{X}_{\mathcal{R}}, X_G^j, k\}}{\arg\max} \log \mathcal{L}(\mathbf{r_o} | \mathbf{X}_{\mathcal{R}}, X_{T_x} = X_G^j, N = k) \\ &= \underset{\{\mathbf{X}_{\mathcal{R}}, X_G^j, k\}}{\arg\max} \sum_{\theta_o \in [-180°, 180°)} \log \mathbb{P}(r'_{\theta_o} = r_{\theta_o} | \mathbf{X}_{\mathcal{R}}, X_{T_x} = X_G^j, N = k)\end{aligned} \tag{6}$$

where $\mathbf{X}_{\mathcal{R}} \subset \mathbf{X}_G^k$ is a $k$ dimensional vector with $n_G^{2k}$ possible values for $N = k$ and $j \in \{1, n_G^2\}$.

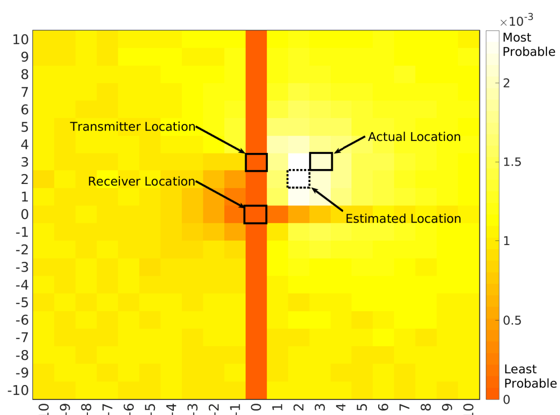


**Figure 2: Probability heat map of different possible positions of the reflector for known position of transmitter** $(0, 3)$ **and receiver** $(0, 0)$**.**

# 4 PERFORMANCE EVALUATIONS

## 4.1 Simulation Experiment Results

To verify the localization performance of the MLE algorithm, we performed a set of simulation experiments. The simulated RSSI data were generated based on the standard path loss model [16] with log normal fading noise $\Psi$ with a maximum standard deviation of $\sigma^2 = 5$. The path loss exponent, $\gamma$, was set to be 1.856 in order to match our real experiments, detailed later. The transmitter power $P_{TX}$ is set to be $7dBm$ to match the maximum transmission power of Openmotes [12] used in real experiments. To simulate the resultant RSSI for an environment with reflecting objects ($\mathbf{X}_{\mathcal{R}}$), the simulated RSSI values for the transmitter was superposed with simulated multipath RSSI values contributed by each of the reflective surfaces. We use a granularity of $\delta = 1.8°$ to match the granularity of our real system implementation. The grid granularity, $d_G$, is set to be 1m since the standard RSSI based localization errors are in the order of meters. The distance traveled by multipath components are calculated using cosine rule as follows: $d_r = \sqrt{d^2 + d_o^2 - 2.d.d_o.cos(\theta_o)} + d_o$ where $d$ is the distance between the transmitter and the receiver, $d_o$ is the distance between the reflector and the receiver, and $\theta_o$ is the angle formed by the transmitter and the reflecting object, at the receiver (illustrated in Figure 1).

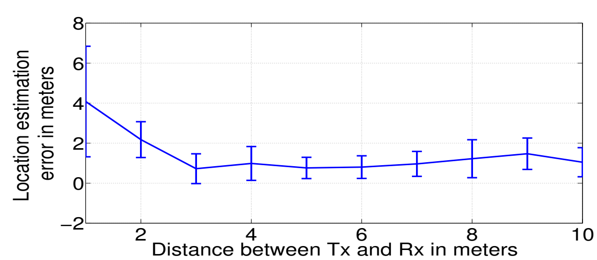


**Figure 3: Error Statistics for varying distance between** $T_x$ **and** $R_x$ **while the reflector is kept fixed at** $(3, 3)$

We performed the simulation experiment for a single reflector with known location of the transmitter as well as with unknown location of the transmitter. In Figure 2, we present the probability heat map for a single reflector with known transmitter location. In this instance, the transmitter was placed at $(0, 3)$ while the receiver was located at $(0, 0)$. The reflector was placed at $(3, 3)$. Figure 2 shows that the grid locations close to the actual position of the reflector have higher probability according to MLE than any other grid locations. To further analyze the performance, we vary the position of the reflector as well as the transmitter. In Figure 3, we present the error performance statistics for a fixed location of the reflector at $(3, 3)$ while the distance to the transmitter, $d$, is varied from 1m to 10m. Figure 3 illustrates that the performance of the MLE is worse when the transmitter is much closer to the receiver than the reflector i.e., $d << d_o$. In this case, the power of the reflected signal is much lower than the direct path power from a nearby transmitter. As the distance between the transmitter and the receiver ($d$) increases, the error decreases. Based on this observation, we hypothesize that MLE detection performance improves when direct path power and the multipath power are comparable, and deteriorates when the multipath power is much smaller compared to the direct path power. To further verify this hypothesis, we fixed the location of the transmitter at $(0, 3)$ and varied the distance between the receiver and the reflector ($d_o$) from 1m to 10m. The experiment outcomes, illustrated in Figure 4, shows that with increasing distance to the reflector, the performance prominently deteriorate. This validates our hypothesis.

We also performed a small set of experiments with unknown locations of the transmitter. In this set of experiments, the distance between $T_x$ and $R_x$ was varied while the reflector is kept static at $(2, 2)$. The results are summarized in Table 1. These results concur with the earlier results i.e., when the distance $d$ is comparable or higher than the distance $d_o$, the performance of the MLE based estimation is better. It also shows that the error in the detection of the transmitter location is very small ($< 1m$) in all three cases. Experiments for higher number of reflectors is left as a future work due to time-constraints.

**Table 1: Simulation experiment based error statistics (in meters) for unknown transmitter and unknown reflector**

| $T_x - R_x$ Distance (d) | (Mean, Std) of Errors in $T_x$ location | (Mean, Std) of Errors in $R_x$ location |
|---|---|---|
| 1m | (0, 0) | (3.7708, 3.9555) |
| 2m | (0.4, 0.2667) | (2.2494, 0.5166) |
| 3m | (0.7, 0.4556) | (2.5891, 1.0524) |

## 4.2 Real Experiment Results

To test the practicality of the concept, we also developed a hardware prototype of the system, mounted on top of a robot as illustrated in Figure 5. In the developed system, the receiver module consists of a stepper motor, a stepper motor driver, and an embedded sensor node (Openmote [12]) with an external directional antenna. Openmote is an open hardware platform for implementing open source IoT standard protocols. It consists of a TI 32-bit CC2538 @ 32 MHz with 512KB Flash memory, 32KB RAM, and 2.4GHz IEEE 802.15.4-based Transceiver connected via SMA plug. The directional antenna used is Rosewill Model RNX-AD7D that works for both WiFi bands, i.e., 2.4MHz and 5GHz, with maximum Gain of 5dBi and 7dBi, respectively. The Half Power Beam Widths (HPBW) of the antenna are 70° and 50° for 2.4GHz and 5GHz, respectively. The whole idea of using an antenna with such a wide directional HPBW is to demonstrate that the system can be built with cheap, off-the-shelf antennas instead of costly, custom solutions. In this system,

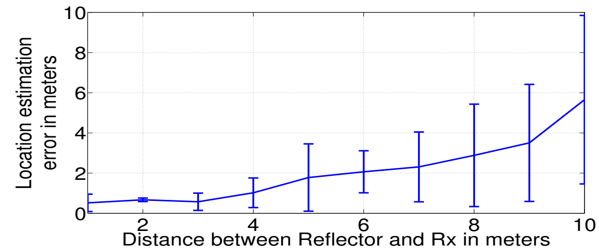


**Figure 4: Error statistics for varying distance to the reflector from the receiver while the $T_x$ is kept fixed at $(0, 3)$**

the transceiver of the Openmote is switched with the directional antenna. The Openmote with the directional antenna is mounted on a stepper motor using a mounting plate. The stepper motor used for this purpose is a Nema 17, 4-wire bipolar motor of dimension 1.65"x1.65"x1.57" with step size of 1.8° (200 steps/rev). The Rated current is 2A and the rated resistance is 1.1 Ohms. The motor driver used for this purpose is an EasyDriver - Stepper Motor Driver. We use an mbed NXP LPC1768 for precise control of the motor via the Easydriver. The Openmote sends interrupts to the mbed whenever it collects a RSSI measurement and sends the data through serial communication, whereas the mbed generates proper output to turn the motor periodically by one step, i.e., 1.8°. In our implementation, the rotation directions are alternated in consecutive cycles in order to avoid wire twisting issues. The transmitter is this case is a standalone Openmote. For programming of the Openmotes, we used the open source RIOT OS [13] for low power IoT Devices. The rotating antenna platform completes a full scanning in $2s$ to generate the output RSSI vector, $\mathbf{r_o}$. This RSSI data is then fed to a computer via USB for processing. The size of the entire robot is roughly 8"x8"x8".

**Figure 5: Real System Prototype**

With this system, we collected a set of real measurement data via a range of experiments in a controlled anechoic chamber environment with precise control over the reflector locations. The anechoic chamber prevents uncontrollable reflection of radio waves from any surrounding surface not accounted for. The transmitter was placed at $\approx 0°$ with respect to the receiver antenna assembly. We performed the experiment for three sets of configurations with a single reflector. We used a metallic plate as a reflector with the center located at $\approx (1, 1)$ in the 2D space illustrated in the problem formulation. An illustration of the experiment is presented in Figure 1. For each configuration, we collected 100 sets of RSSI vector. We fed this vectors to a MATLAB code to process the data and estimate the location of the reflector. We varied the distance

$d$ between the transmitter and the receiver to be 1m, 2m, and 3m, respectively. The granularity of the search grid, $d_G$, is set to be 0.5m in this set of experiments. For this set of experiments, we calculated the path loss exponent ($\gamma = 1.856$) and the constants in Eqn (2) based on some initial RSSI measurements. We use a transmission power of $P_{T_x} = 7dBm$ which is the maximum transmission power of the Openmote. Note that, in these experiments some extra unaccountable errors are still introduced by the fact that the reflector is not a point source. The error statistics for this set of experiments is presented in Table 2. The results suggest that the proposed system performs well with error in the order of meters. The similar performance in all three cases in justified by the fact that $d$ and $d_o$ are comparable for all three cases. With this system, one can potentially achieve reasonable mapping performance upto $\approx 6m$ separations among the transmitter, the receiver, and the reflectors.

**Table 2: Error statistics for real-world experiments in meters**

| $T_x - R_x$ Distance ($d$) | Mean of Errors | Std of Errors |
|---|---|---|
| 1m | 0.9m | 0.1m |
| 2m | 1.4m | 0.1m |
| 3m | 0.7m | 0.2m |

## 5 DISCUSSIONS AND FUTURE WORKS

In this paper, we have presented a proof of concept method of employing a single RF transmitter and a single RF receiver toward localizing reflecting objects which can be potentially extended to a full-fledged mapping of the environment. We use a MLE based estimation method for this purpose. Based on some base simulation and real-world experiments, we demonstrated that the proposed system works with reasonable performance for a single unknown reflector with both known and unknown location of the transmitter. However, the MLE based approach is definitely not scalable as the search space increases exponentially with number of unknowns. Thus, in our ongoing work, we are investigating a more scalable and efficient approach with similar performance guarantees. Next, we briefly introduce our ongoing work. We model the system as a linear system with system equations as follows:

$$\mathbf{r_o} = \mathcal{G} \cdot \mathbf{P} \tag{7}$$

$$\begin{bmatrix} r_0 \\ r_{1.8} \\ \vdots \\ r_{-1.8} \end{bmatrix} = \begin{bmatrix} g_{-180} & \cdots & g_0 & \cdots & g_{178.2} \\ g_{178.2} & \cdots & g_{-1.8} & \cdots & g_{176.4} \\ \vdots & \vdots & \vdots & \vdots & \vdots \\ g_{-178.2} & \cdots & g_{1.8} & \cdots & g_{-180} \end{bmatrix} \begin{bmatrix} P_{-180} \\ \vdots \\ P_{178.2} \end{bmatrix} \tag{8}$$

where $r_\theta$ is the value of RSSI when antenna orientation is $\theta^o$ with respect to the +ve y axis, $g_\theta$ is the angular gain of the antenna for direction $\theta$, and $P_\theta$ is the received power of the multi-path component along the $\theta$ angle. Now, in absence of fading, we can exactly calculate the multipath components using (8) as the gain matrix $\mathcal{G}$ is known as well as the measured RSSI vector, $\mathbf{r_o}$. However, in presence of fading, the linear equation does not hold and becomes:

$$\mathbf{r_o} = \mathcal{G} \cdot \mathbf{\Psi} \cdot \mathbf{P} \tag{9}$$

where the unknown $\mathbf{\Psi} = diag(\psi_1, \psi_2, \cdots, \psi_{200})$ accounts for the fading of each multipath component. Solving this equation, ideally, would give us all the multipath components. Once the multipath vector is calculated, the corresponding path distances $d_{\theta_i}$ (which is actually the total distance travelled by the reflected signals) of each of the multipath component can be calculated as: $d_{\theta_i} = C'.P_{\theta_i}^{-1/\gamma}$ where $C'$ is some constant. The smallest value of $d_{\theta_i}$ will correspond to the direct path distance, $d$. Say, the corresponding direction is $\theta_t$. For each of the remaining multipath components with power $P_{\theta_i}$, we obtain the most likely distance between the receiver and the reflector, $d_o$, by comparing the position of the reflector that would generate a reflected path closest to $d_{\theta_i}$ as: $\arg\min_{d_o} \left| d_{\theta_i} - \left( d_o + \sqrt{({d_o}^2 + d^2 - 2.d.d_o.cos(\theta_o))} \right) \right|$ where $\theta_o = \theta_i - \theta_t$ is the angle formed by the reflector and the transmitter at the receiver. With this technique we can potentially perform scalable finer granularity search to make the system more conformed towards real world scenarios with non-discrete spaces. However, to solve for the vector $\mathbf{P}$, we need to employ some sophisticated method such as compressible sampling. We verified that the traditional solutions such as Min-Square Approximation approach doesn't perform well. The algorithm development for solving Eqn (9) is one of our ongoing work. Moreover, our current estimation approach is implemented on MATLAB which requires significant computation power. Thus, another future direction is to implement a low complexity estimation algorithm on a commercially available low processing power device such as Openmote. Lastly, extending this framework to a controlled robotic receiver to improve the performance by collecting measurements at more receive locations and to map the whole environment is another direction of future work.

## REFERENCES


[1] Fadel Adib, Chen-Yu Hsu, Hongzi Mao, Dina Katabi, and Frédo Durand. 2015. Capturing the human figure through a wall. *ACM TOG* 34, 6 (2015), 219.
[2] Fadel Adib, Zachary Kabelac, Dina Katabi, and Robert C Miller. 2014. 3D Tracking via Body Radio Reflections. In *NSDI, 2014*.
[3] Sundar Aditya, Andreas F Molisch, and Hatim Behairy. 2015. Bayesian multi-target localization using blocking statistics in multipath environments. In *IEEE ICCW, 2015*.
[4] John Aldrich et al. 1997. RA Fisher and the making of maximum likelihood 1912-1922. *Statist. Sci.* 12, 3 (1997), 162–176.
[5] Kevin Chetty, Graeme E Smith, and Karl Woodbridge. 2012. Through-the-wall sensing of personnel using passive bistatic wifi radar at standoff distances. *IEEE Transactions on Geoscience and Remote Sensing* 50, 4 (2012), 1218–1226.
[6] Berk Gulmezoglu, Mehmet Burak Guldogan, and Sinan Gezici. 2015. Multiperson tracking with a network of ultrawideband radar sensors based on Gaussian mixture PHD filters. *IEEE Sensors Journal* 15, 4 (2015), 2227–2237.
[7] Chitra R Karanam and Yasamin Mostofi. 2017. 3D through-wall imaging with unmanned aerial vehicles using wifi. In *ACM/IEEE IPSN, 2017*.
[8] Swarun Kumar, Ezzeldin Hamed, Dina Katabi, and Li Erran Li. 2014. LTE radio analytics made easy and accessible. In *ACM SIGCOMM, 2014*.
[9] Hui Liu, Houshang Darabi, Pat Banerjee, and Jing Liu. 2007. Survey of wireless indoor positioning techniques and systems. *IEEE SMC, Part C (Applications and Reviews)* 37, 6 (2007), 1067–1080.
[10] Yasamin Mostofi. 2011. Compressive cooperative sensing and mapping in mobile networks. *IEEE TMC* 10, 12 (2011), 1769–1784.
[11] Yasamin Mostofi. 2013. Cooperative wireless-based obstacle/object mapping and see-through capabilities in robotic networks. *IEEE TMC* 12, 5 (2013), 817–829.
[12] Openmote. 2017. http://www.openmote.com/. (2017).
[13] RIOT OS. 2017. https://riot-os.org/. (2017).
[14] Neal Patwari and Joey Wilson. 2010. RF sensor networks for device-free localization: Measurements, models, and algorithms. *Proc. IEEE* 98, 11 (2010), 1961–1973.
[15] Chuan-Chin Pu and Wan-Young Chung. 2008. Mitigation of multipath fading effects to improve indoor RSSI performance. *IEEE Sensors Journal* 8, 11 (2008), 1884–1886.
[16] Theodore S Rappaport et al. 1996. *Wireless communications: principles and practice*. Vol. 2. Prentice Hall PTR New Jersey.
[17] Bo Tan, Kevin Chetty, and Kyle Jamieson. 2017. ThruMapper: Through-Wall Building Tomography with a Single Mapping Robot. In *ACM HotMobile 2017*.
[18] Jue Wang and Dina Katabi. 2013. Dude, where's my card?: RFID positioning that works with multipath and non-line of sight. *ACM SIGCOMM Computer Communication Review* 43, 4 (2013), 51–62.
[19] Nicholas J Willis. 2005. *Bistatic radar*. Vol. 2. SciTech Publishing.